nature chemistry

SUPPLEMENTARY INFORMATION

https://doi.org/10.1038/s41557-020-0494-4

In the format provided by the authors and unedited.

Emergence of light-driven protometabolism on recruitment of a photocatalytic cofactor by a self-replicator

Guillermo Monreal Santiago, Kai Liu, Wesley R. Browne and Sijbren Otto ✉

Centre for Systems Chemistry, Stratingh Institute, University of Groningen, Groningen, the Netherlands. ✉e-mail: s.otto@rug.nl

Supplementary information for:

Emergence of light-driven protometabolism upon recruitment of a photocatalytic cofactor by a self-replicator

Authors: Guillermo Monreal Santiago[1], Kai Liu[1], Wesley R. Browne[1], Sijbren Otto[1*].

Affiliations:

[1]Centre for Systems Chemistry, Stratingh Institute, University of Groningen, Nijenborgh 4, 9747 AG Groningen, Netherlands.

[*]Corresponding author. Email: s.otto@rug.nl

Contents:

Samples containing **2**		
Time (min)	%MeCN/ 0.1 % TFA	%H_2O/ 0.1 % TFA
0	10	90
1	10	90
1,3	25	75
3	28	72
11	40	60
11,5	95	5
15	95	5
15,5	10	90
20	10	90

Samples containing **3**		
Time (min)	% MeCN/ 0.1 % TFA	%H_2O/ 0.1 % TFA
0	10	90
1	10	90
1,3	25	75
3	28	72
11	40	60
11,5	95	5
12	95	5
12,5	10	90
17	10	90

Supplementary Table 1

Solvent and gradients used for the UPLC analysis of libraries derived containing **1** and other macrocycles derived from it.

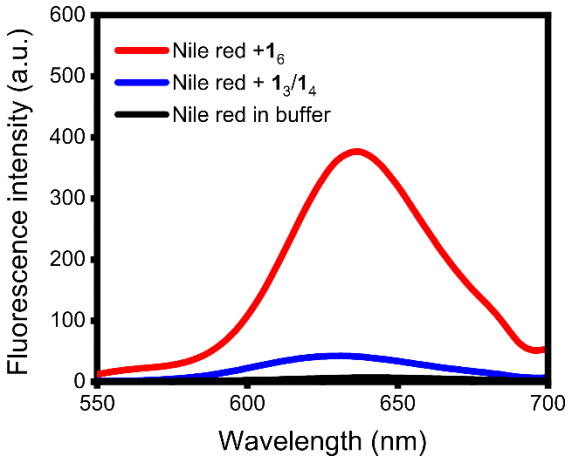

Supplementary Figure 1

Fluorescence of Nile Red (5 μM) in absence and presence of the macrocycles derived from **1** (1.0 mM) with excitation at 530 nm. Enhanced fluorescence indicates the presence of hydrophobic binding sites (*34*).

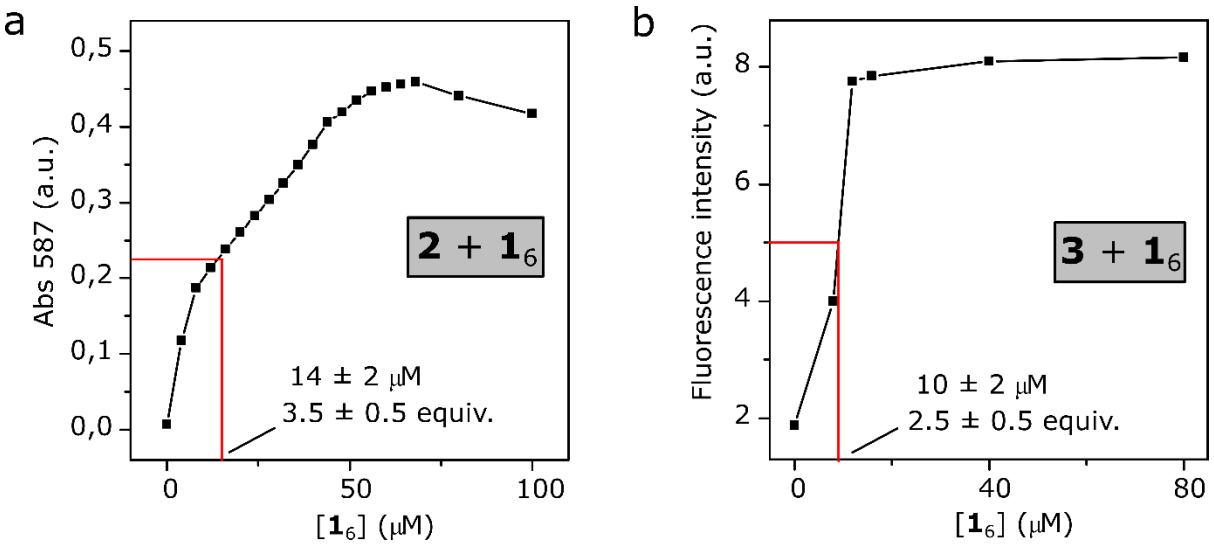

Supplementary Figure 2

Titrations of **2** (4.0 μM, A) and **3** (4.0 μM, B) with increasing amounts of $\mathbf{1}_6$. The red lines indicate the points where 50% of dye molecules are bound to $\mathbf{1}_6$. For **2**, we assume that the point where the J-band intensity is maximum is the point where all molecules are bound, while the decrease with higher concentrations of $\mathbf{1}_6$ is due to an increase of the average distance between molecules of **2**. In the case of **3**, we assume that fluorescence increases as **3** molecules bind to $\mathbf{1}_6$, and its maximum value corresponds to the saturation of $\mathbf{1}_6$. The error represents the difference in [$\mathbf{1}_6$] between two consecutive points of the titration.

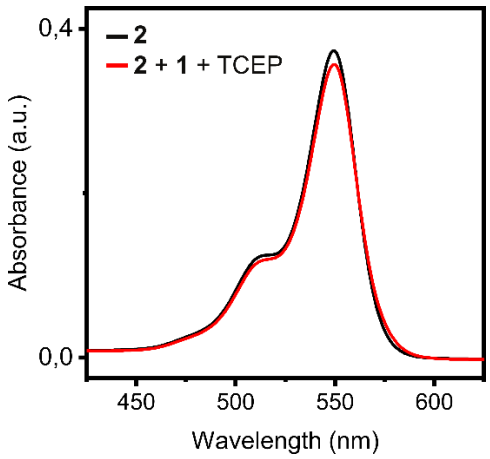

Supplementary Figure 3

Visible absorption spectra of **2** (4.0 μM) in the absence (black) and presence of 80 μM of **1** and 40 μM of TCEP (tris(2-carboxyethyl)phosphine, red). TCEP was added to ensure that **1** was completely reduced, as small amounts of $\mathbf{1}_3$/$\mathbf{1}_4$ could bind to **2** and change the spectrum.

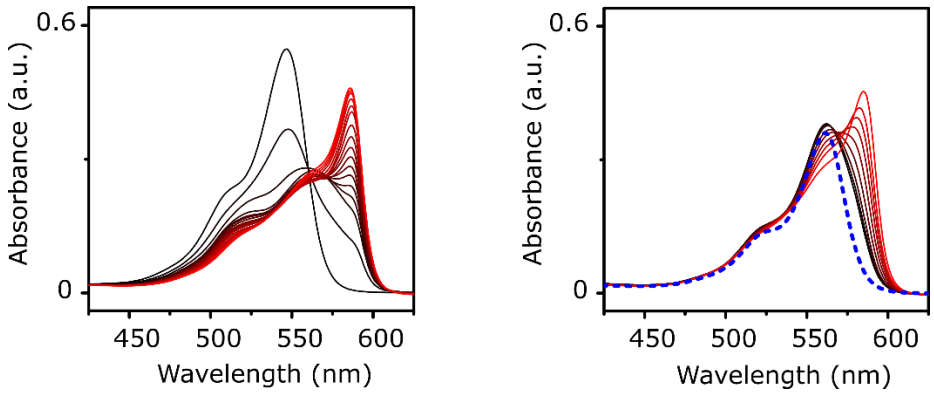

Supplementary Figure 4

Visible absorption spectra of **2** (4.0 μM) in the presence of increasing amounts of $\mathbf{1}_6$. The spectra have been separated in two panels for clarity: Left – from 0 (black) to 16 (red) equivalents of $\mathbf{1}_6$ (in terms of **1**). Right – from 20 (red) to 100 (black) equivalents. In the right panel, the spectrum of **2** (4.0 μM) in presence of 100 equivalents of $\mathbf{1}_3$/$\mathbf{1}_4$ has also been included in a blue dashed line.

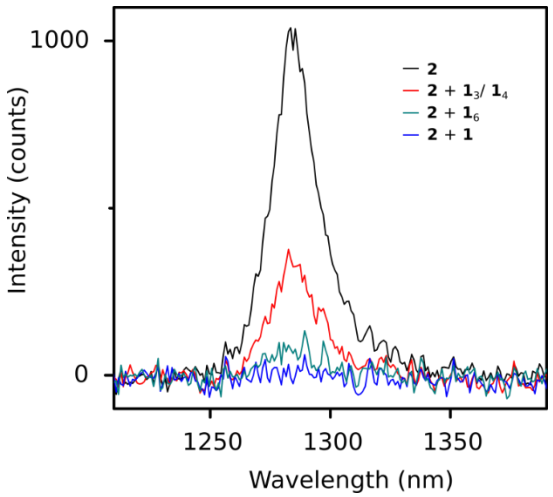

Supplementary Figure 5

$^1O_2$ phosphoresence by sensitisation by **2** in the absence or presence of **1** or macrocycles formed from **1**, monitored through the NIR signal corresponding to $^1O_2$ luminescence (*28*). The spectra were recorded with solutions containing **2** (4.0 μM) and **1**, **1**$_3$/**1**$_4$ or **1**$_6$ (80 μM). Dye **2** retains its activity as photosensitizer in the presence of **1**$_3$/**1**$_4$ or **1**$_6$, albeit with reduced efficiency. In the presence of **1**, as expected, $^1O_2$ emission was not observed as it reacts with the thiols of **1**. The samples were prepared by diluting 4.0 mM stock solutions prepared in borate buffer (pH = 8.2) with D_2O, and irradiated with at 532 nm (45 mW)

Sample	**2**	**2** + **1**$_6$	**2** + **1**$_3$/**1**$_4$
Relative absorbance (532 nm)	1	0.56	0.67
Relative luminescence (integrated)	1	0.1	0.3
$^1O_2$ generation quantum yield, Φ_Δ	0.76 (*29*)	0.1	0.4
Relative absorbance (577 - 603 nm)	1	39.2	6.7
Expected relative photooxidation rate (Abs $_{577\text{-}603}$ * Φ_Δ), normalized to **2**	1	5	3
Experimental relative photooxidation rate	1	2.4	0.9

Supplementary Table 2

Calculated quantum yields of $^1O_2$ generation and expected relative rates of photooxidation with **2** in presence of **2** (4.0 μM) and **1**$_3$/**1**$_4$ or **1**$_6$ (80 μM). The observed oxidation rates in presence of **1**$_3$/**1**$_4$ or **1**$_6$ are around 2-3 times lower than the values expected based only on the effect of the macrocycles on absorbance and quantum yield, indicating that these macrocycles influence the reaction in more ways than by just increasing the absorbance of **2** or decreasing its Φ_Δ.

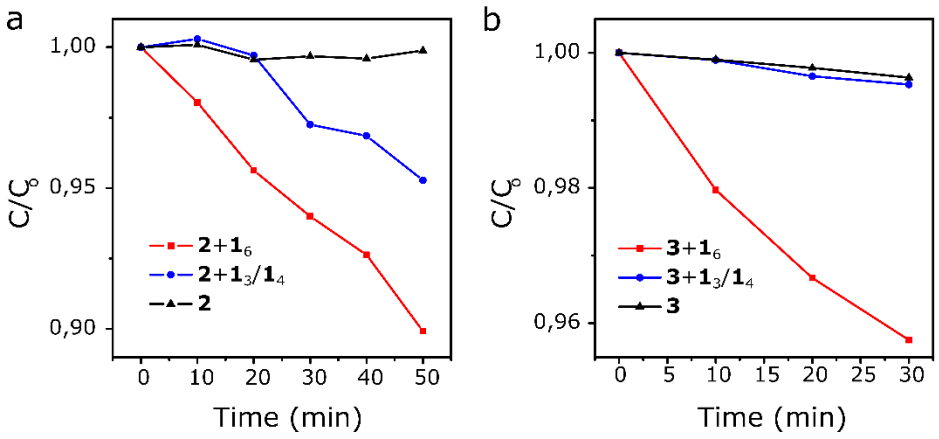

Supplementary Figure 6

Relative $^1O_2$-generation efficiency of **2** (left) or **3** (right) in buffered aqueous solutions in presence of $\mathbf{1}_6$ or $\mathbf{1}_3/\mathbf{1}_4$, measured by using anthracene-9,10-dipropionic acid as a reactive oxygen species probe (*31*). The concentrations used were 10 μM for either **2** or **3**, and 40 μM for the probe. In the sample containing **2** the concentration of $\mathbf{1}_n$ macrocycles was 200 μM (in building blocks **1**) and the irradiation source was a 590 nm LED. In the sample containing **3**, the concentration of $\mathbf{1}_n$ macrocycles was 1.0 mM (in building blocks **1**) and the irradiation source was a halogen lamp. The concentration of probe was measured by UV–vis absorption spectrophotometry, monitoring the absorption at 378 nm. The rates of this reaction follow the same trend as the ones in Fig. 3 ($\mathbf{1}_6$ > $\mathbf{1}_3/\mathbf{1}_4$ > nothing added), although the differences in this case are more pronounced due to the high selectivity of this probe towards $^1O_2$.

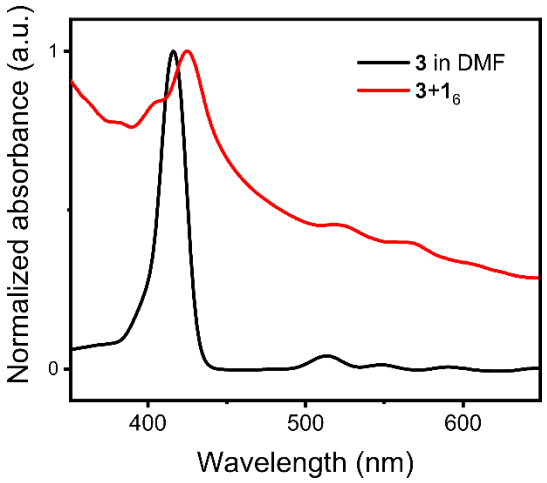

Supplementary Figure 7

Visible absorption spectra of **3** (10 μM) in DMF (black) and in borate buffer, in presence of **1**$_6$ (1.0 mM in **1**, red).

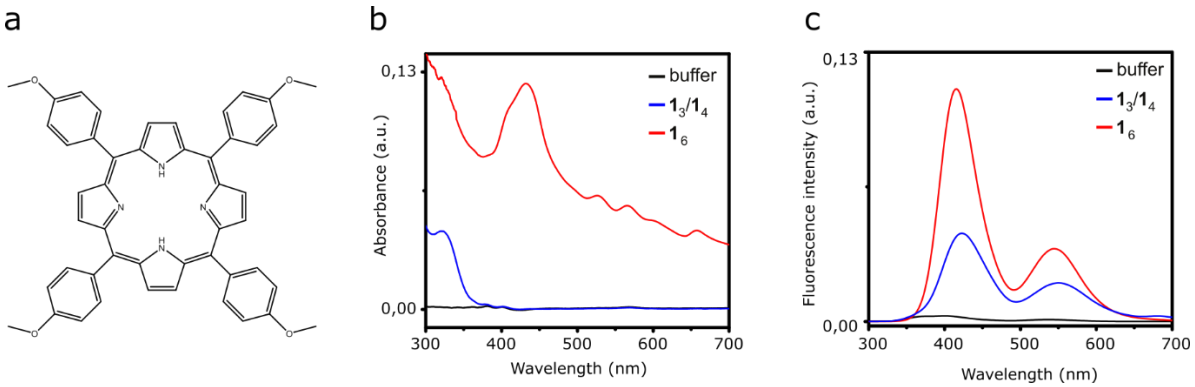

Supplementary Figure 8

a) Molecular structure of 5,10,15,20-tetrakis(4-methoxyphenyl)porphyrin, b) its UV/vis absorption spectra and c) its fluorescence spectra (excitation at 420 nm, concentration = 10 μM) in buffer (black) and in the presence of $\mathbf{1}_3/\mathbf{1}_4$ (1.0 mM in **1**; blue) or $\mathbf{1}_6$ (1.0 mM in **1**; red).

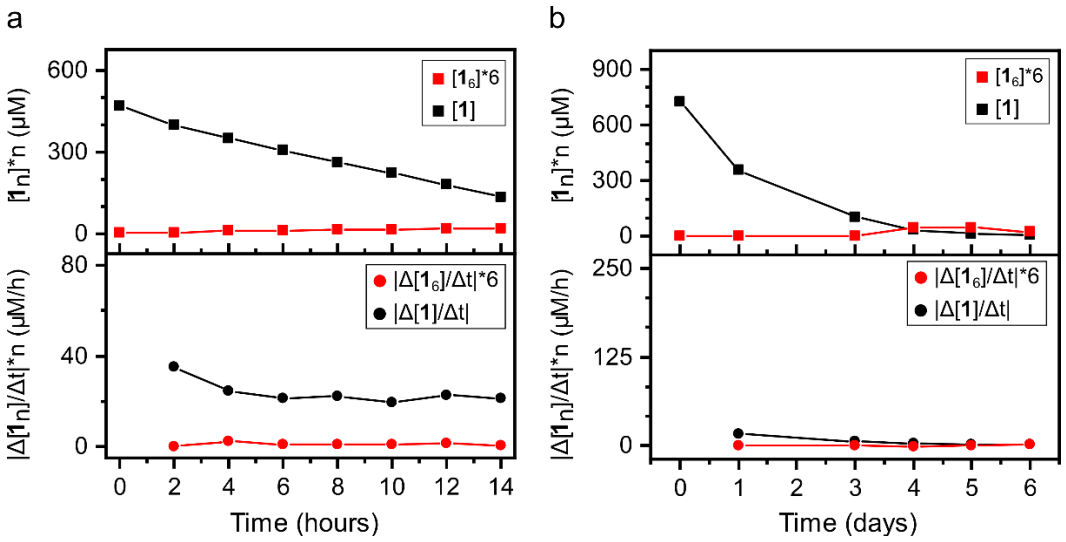

Supplementary Figure 9

Evolution over time of the concentrations of **1** and $\mathbf{1}_6$ in unstirred libraries made from **1** and **2** (a) or **1** and **3** (b). The top halves of the graphs show the concentration of **1** (black squares) and $\mathbf{1}_6$ (red squares, in units of **1**). The bottom halves of the graphs represent the oxidation (black circles) and replication (red circles) rates in the system, calculated by numerical differentiation of the curves in the top halves. Both libraries were prepared exactly as their equivalents in Figure 4, but they were not stirred.

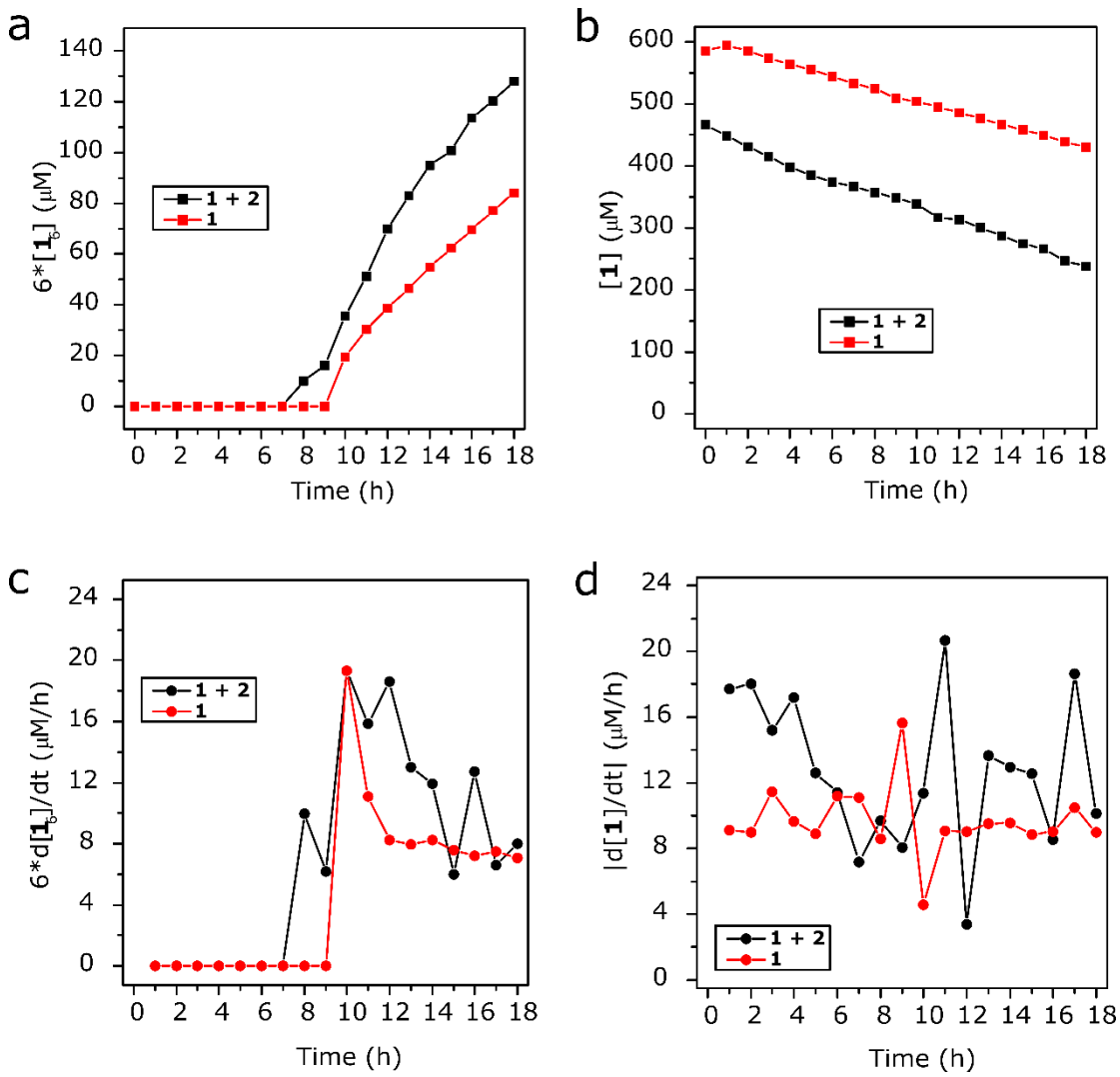

Supplementary Figure 10

The presence of **2** does not significantly affect the system in absence of irradiation. Concentrations of $\mathbf{1}_6$ (a) and **1** (b), and replication (c) and oxidation (d) rates in stirred unirradiated libraries of **1** (~500 μM), in presence (black) or absence (red) of **2** (1.0 μM). The small differences in the time point at which $\mathbf{1}_6$ emerges reflects the statistical fluctuation that is typically observed for the stochastic fibre nucleation process.

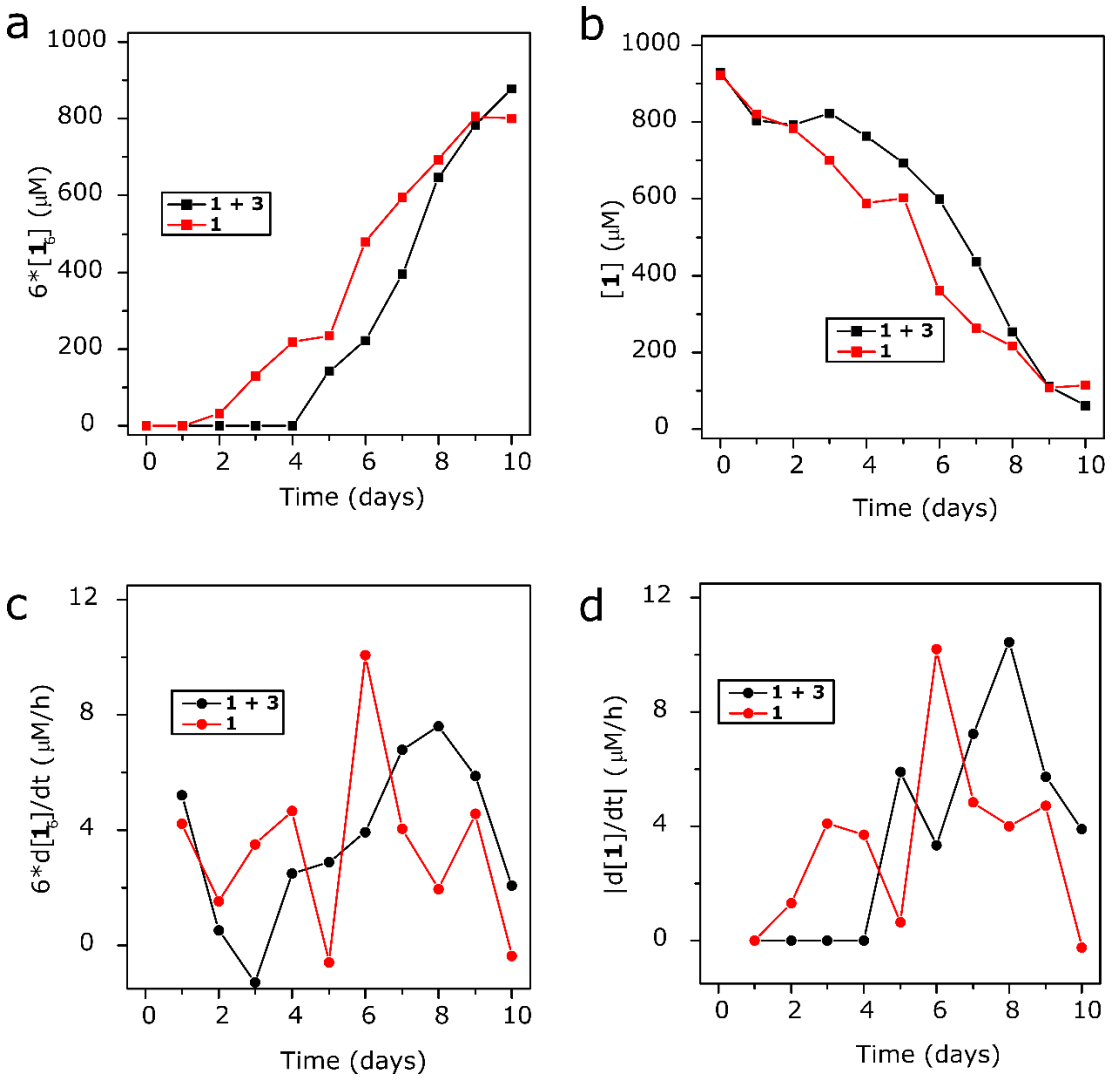

Supplementary Figure 11

The presence of **3** does not significantly affect the system in absence of irradiation. Concentrations of $\mathbf{1}_6$ (a) and **1** (b), and replication (c) and oxidation (d) rates in stirred unirradiated libraries of **1** (1.0 mM), in presence (black) or absence (red) of **3** (5.0 μM). The small differences in the time point at which $\mathbf{1}_6$ emerges reflects the statistical fluctuation that is typically observed for the stochastic fibre nucleation process.

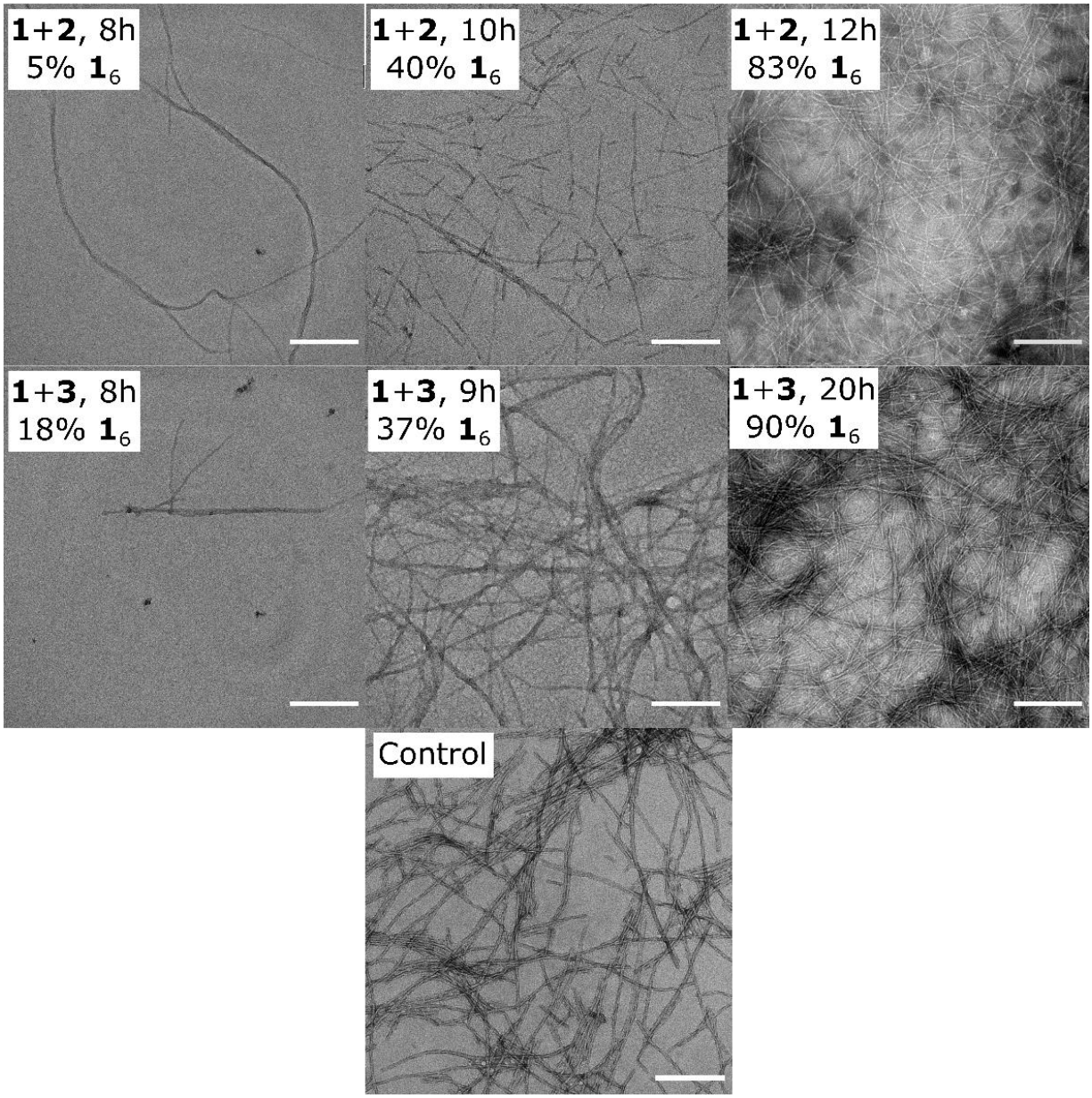

Supplementary Figure 12

Self-assembled structures of $\mathbf{1}_6$ formed upon photooxidation catalysed by **2** or **3**. Libraries with dyes were prepared under the same conditions as in Fig. 4, and aliquots were taken and analyzed by UPLC and negative staining transmission electron microscopy (TEM) at different times. No morphological differences were observed between the fibres formed in presence of dyes and the ones formed by oxidation with air at 40 ºC (control). No differences were observed over time either (except that there tends to be a higher density of fibres as the concentration of $\mathbf{1}_6$ increases, however this cannot be quantified since it depends on drying and the region of the grid imaged). The scale bars correspond to 200 nm.

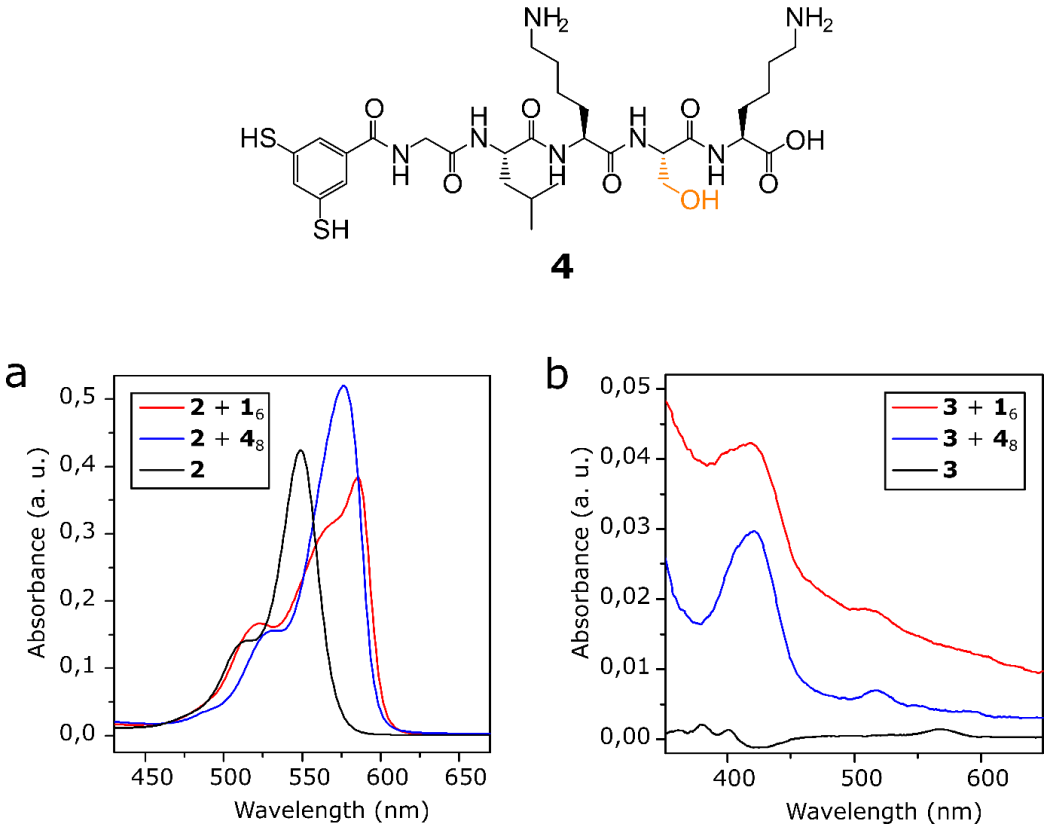

Supplementary Figure 13

Small changes in the replicator structure change the binding of dyes. UV spectra of **2** (a) or **3** (b) in presence of replicators $\mathbf{1}_6$ and $\mathbf{4}_8$ *(32)*. The concentration of dye was 4.0 µM, and the concentration of replicator was 80 µM in (a) and 200 µM in (b) (in units of dithiol building blocks). The structure of **4** is shown at the top, highlighting its differences with the structure of **1**.

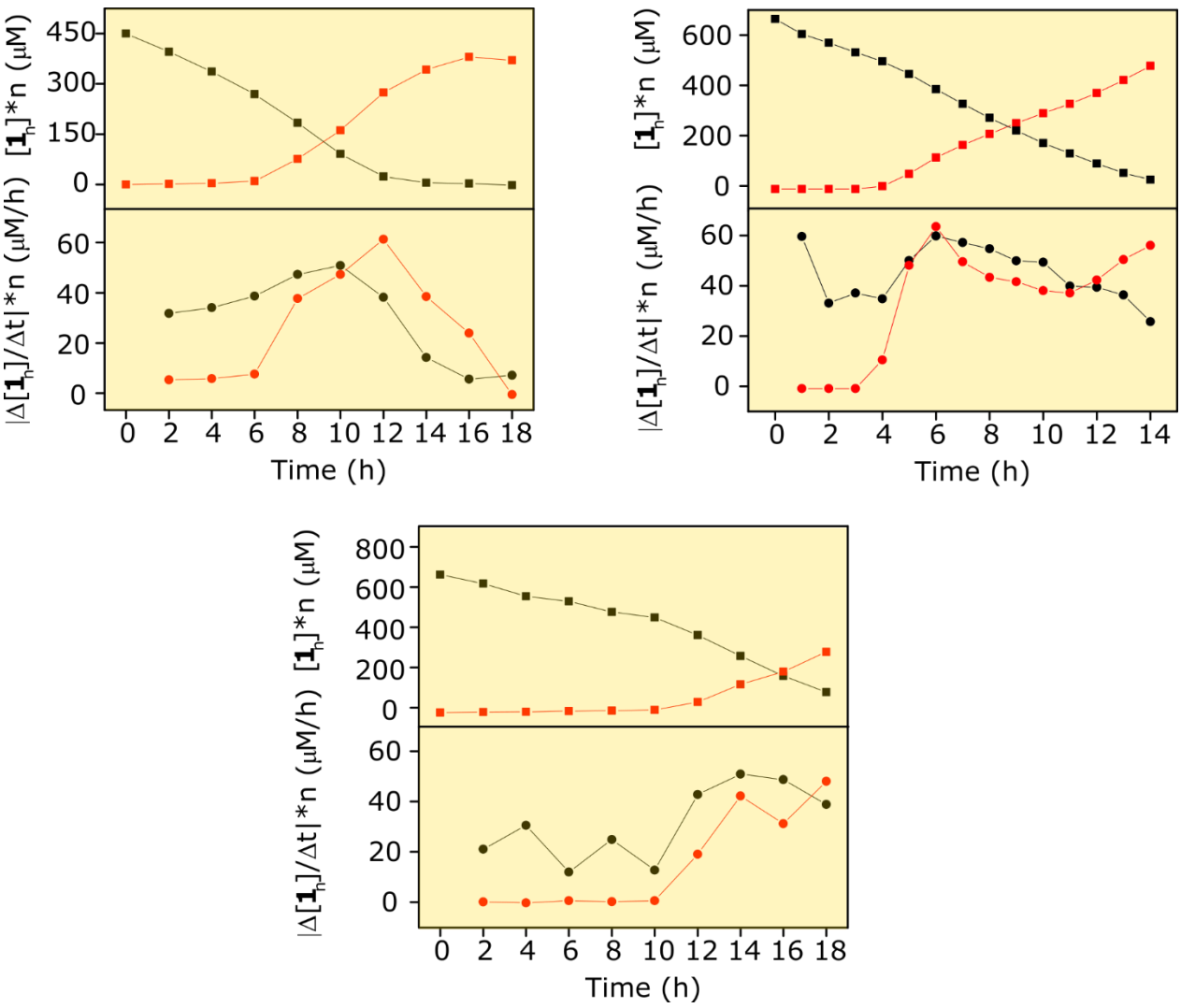

Supplementary Figure 14

Evolution over time of the concentrations of **1** and $\mathbf{1}_6$ in three repeats of the same experiment, containing **1** and **2**. The top halves of the graphs show the concentration of **1** (black squares) and $\mathbf{1}_6$ (red squares, in **1** units). The bottom halves of the graphs represent the oxidation (black circles) and replication (red circles) rates in the system, calculated by numerical differentiation of the two curves in the top halves. All libraries were prepared using the same conditions as for the experiments shown in Figure 4a.

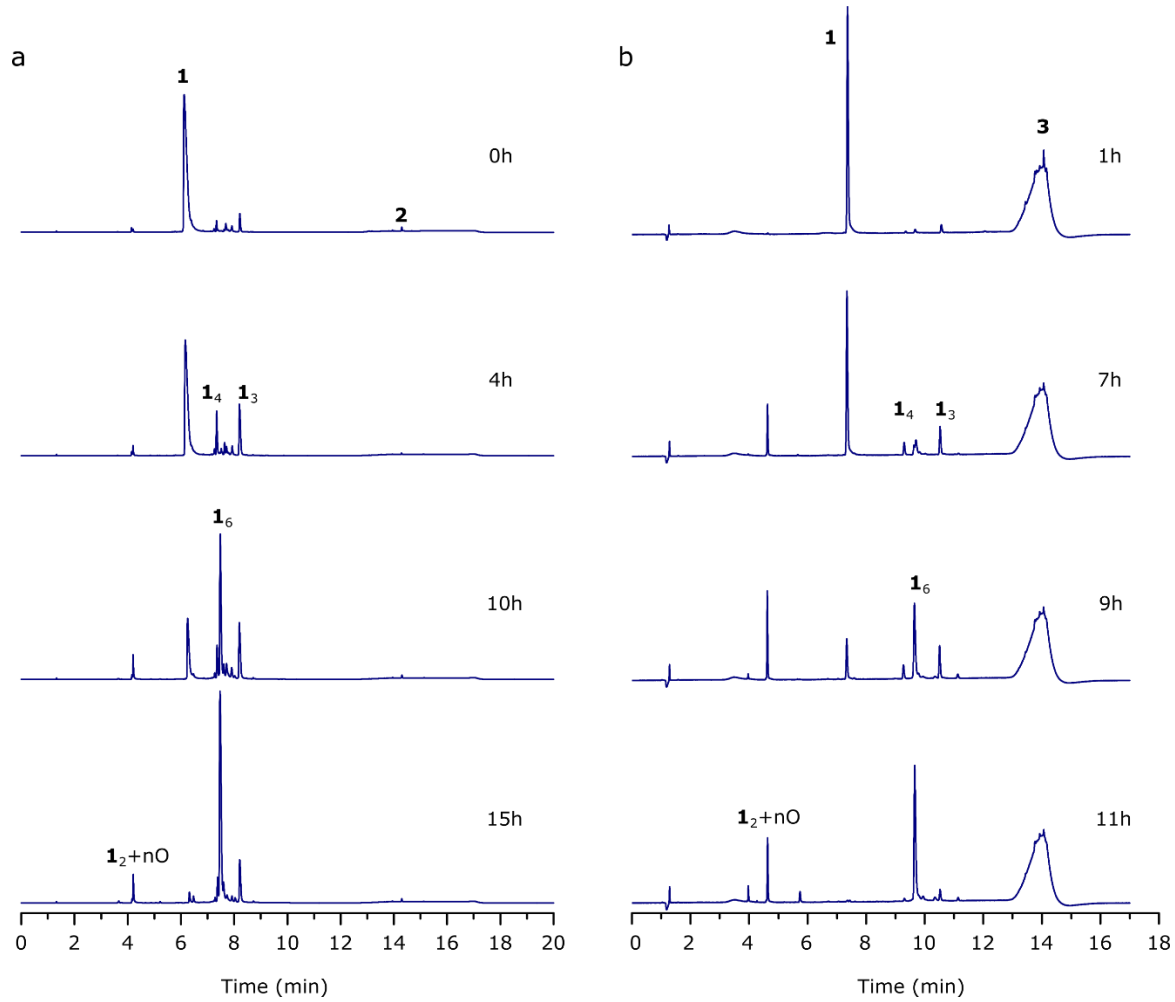

Supplementary Figure 15

UPLC chromatograms (monitored at 254 nm) of typical stirred libraries of (a) **1** + **2** under 590 nm irradiation, kept at 40 °C, and (b) **1** + **3**, irradiated with a halogen lamp at room temperature (in the same conditions as the ones in Figures 4a and 4c, respectively). Building block **1**, and the disulfides formed by its oxidation, elute between 6 and 12 minutes and have similar molar absorptivities at 254 nm (*19*). The evolution over time of the total peak area between 6 and 12 minutes is shown in Supplementary Figure 16, and the mass spectrum corresponding to the peak at ~4 minutes is shown in Supplementary Figure 17.

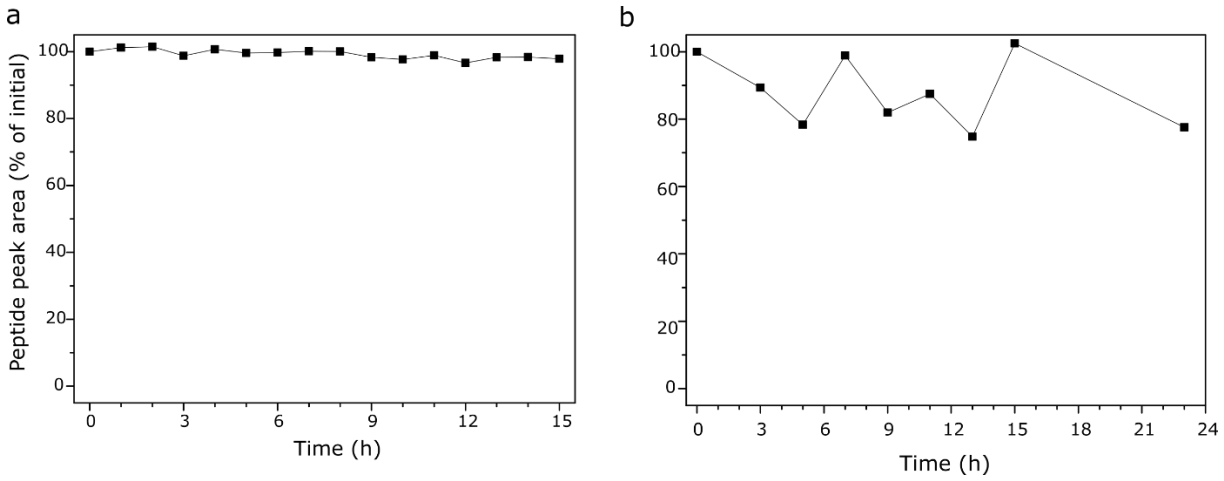

Supplementary Figure 16

Peak area between 6 and 12 minutes (corresponding to **1** and its disulfide-based derivatives) in successive chromatograms of irradiated libraries (a) containing **1** + **2**, kept at 40 °C and (b) containing **1** + **3** and kept at room temperature (the libraries were prepared using the same conditions as the ones in Figure 4). The values are represented as % of the initial peak area, showing that in both cases the amount of oxidation products other than disulfides is negligible. The noise in the sample containing **3** is higher due to sampling (see Methods).

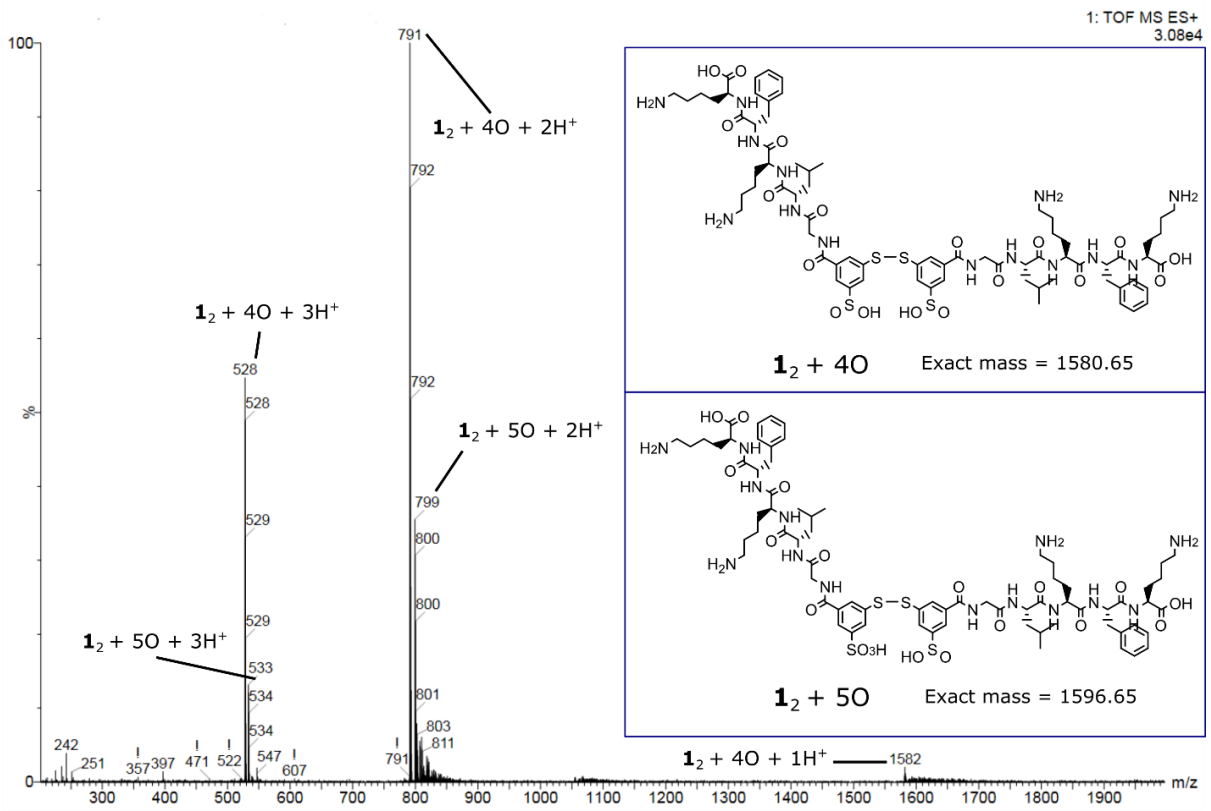

Supplementary Figure 17

Mass spectrum of the peak formed in photooxidized libraries, with retention time ~4 minutes. Possible isomers of the ions that can be detected.